chemosensors

Article

Characterization of a Novel Polypyrrole (PPy) Conductive Polymer Coated Patterned Vertical CNT (pvCNT) Dry ECG Electrode

Mohammad Abu-Saude * and Bashir I. Morshed *

Department of Electrical and Computer Engineering, The University of Memphis, Memphis, TN 38152, USA
* Correspondence: mbusaude@memphis.edu (M.A.); bmorshed@memphis.edu (B.I.M.)

Received: 13 June 2018; Accepted: 10 July 2018; Published: 17 July 2018

Abstract: Conventional electrode-based technologies, such as the electrocardiogram (ECG), capture physiological signals using an electrolyte solution or gel that evaporates shortly after exposure, resulting in a decrease in the quality of the signal. Previously, we reported a novel dry impedimetric electrode using patterned vertically-aligned Carbon NanoTubes (pvCNT) for biopotential measurement applications. The mechanical adhesion strength of the pvCNT electrode to the substrate was weak, hence, we have improved this electrode using a thin coating of the conductive polymer polypyrrole (PPy) that strengthens its mechanical properties. Multiwall CNTs were grown vertically on a circular stainless-steel disc ($\varnothing$ = 10 mm) substrate of 50 µm thickness forming patterned pillars on a square base (100 µm $\times$ 100 µm) with an inter-pillar spacing of 200 µm and height up to 1.5 mm. The PPy coating procedure involves applying 10 µL of PPy mixed with 70% ethyl alcohol solution and rapid drying at 300 °C using a hot air gun at a distance of 10 cm. A comparative study demonstrated that the coated pvCNT had higher impedance compared to a non-coated pvCNT but lower impedance compared to the standard gel electrode. The PPy-coated pvCNT had comparable signal capture quality but stronger mechanical adhesion to the substrate.

Keywords: dry ECG electrode; impedimetric electrode; carbon nanotube (CNT); pvCNT electrode; polypyrrole (PPy) coating

1. Introduction

Physiological signals, e.g., electrocardiogram (ECG/EKG), electroencephalogram (EEG), electromyogram (EMG), and galvanic skin response (GSR), play a vital role in health monitoring and clinical diagnoses, as well as non-clinical applications, such as neurofeedback and brain–computer interface (BCI) [1–4]. Impedimetric electrodes are required to collect these body signals. Conventional wet electrodes, such as Ag/AgCl electrodes, use a saline- or gel-based electrolyte to decrease the contact impedance and artifacts due to motion and to increase the dielectric constant between the skin surface and the electrode [5]. The gel reduces the resistance between the surface of the metal part of the electrode and the skin below the stratum corneum (SC) layer. These sensors only operate well for a short duration because of gradual degradation of conductivity as the electrode interface impedance deteriorates over time, due to evaporation, leading to a degradation in signal quality [6–12]. Wet or gel electrode applications also require inconvenient skin preparation whereby an expert is typically required to remove dirt, skin debris, and oil from the skin surface. Furthermore, the gel has been observed to be a source of the contact noise [12] and could potentially cause an allergic reaction in the patient. Wet or gel electrodes lead to detrimental reliability over a long period; hence, the current practice is to periodically replace the electrodes, burdening the user and the operator-in-the-loop (e.g., clinician). These technological barriers pose problems for continuous health and wellness monitoring that require neuro-physiological signal monitoring for prolonged periods [5,13,14]. Furthermore, the half-cell noise appears at the interface between the gel and the electrode due to diffusion of the gel into the top layer of the skin [12]. The wet and gel Ag/AgCl electrodes are widely used for clinical and research purposes. However, wet electrodes dry within a few hours while gel electrodes only work up to 10 h. Hence, these electrodes are not suitable for long durations and continuous monitoring. These drawbacks have motivated researchers to develop alternatives, such as dry impedimetric electrodes.

Dry electrodes are designed to operate and record biopotential signals without explicit conductive gel and skin preparation and allow for long duration impedimetric sensing without degradation of impedances. However, this method suffers from high interfacing impedances, interfacial potential, contact surface, and noise [6–8]. Planar flexible dry electrodes have been developed for long-term ECG monitoring by depositing gold on polydimethylsiloxane (PDMS) films using plasma treatment [15,16] or using polypyrrole (PPy) thin film on a copper substrate [17], however these suffer poor skin-contact electrical connectivity. Microneedle dry electrodes fabricated using the process of the microelectromechanical system (MEMS) [18] have recently generated significant interest for use in long-term biopotential signal recording. Silicon microneedle-based dry electrodes for biopotential monitoring are made by etching the wafer and depositing metal in both sides in an array pattern [19]. Flexible microneedle-based electrodes were developed using PDMS with different pins, which pass through hair, but suffer from high contact impedance [16]. Fixable metal-coated polymer bristle-sensors are another promising type of dry electrode that is able to penetrate through a thick layer of hair and has low impedance; however, they are large and uncomfortable for long-term usage [20]. Some dry electrodes that have comfortable interfaces such as conductive sponge [21], ceramic [22], and foam [6] suffer from a high impedance (~10 kΩ) at low frequencies (~100 Hz). Silver ink used in Inkjet-based dry electrodes shows low impedances but the surface connectivity issues remain [23]. Non-contact electrodes are very sensitive to any motion of the electrode with respect to the body as the capacitance dramatically changes by a factor of 10 when the electrode moves 100 μm vertically [24,25]. Textile electrodes were developed by coating cotton woven fabrics with polypyrrole [26] and synthesizing conductive fabrics with graphene cladding [27] which resulted in a good quality ECG signal. There is significant ongoing research looking into developing a high-performance dry electrode [28,29].

Carbon nanotubes (CNTs) are a new technology that has been utilized to develop some biosensors. Multiwall CNTs (MWCNTs) are highly conductive and therefore practically suitable for developing biopotential electrodes [30,31]. Purified CNTs are stable over a long period of time [32]. Some studies have shown that, at low concentration, CNTs have relatively low toxicity [33–35]. CNT-based electrodes display unique properties that provide reliable interfacing to biopotential signals and are desirable due to their ability to penetrate biological membranes [36,37]. Carbon nanotube (CNT)/polydimethylsiloxane (PDMS) or polypyrrole (PPy) composite-based dry ECG electrodes showed long-term wearable monitoring capability and robustness to motion and sweat. However, these electrodes suffered from poor electrical conductivity for the planar top surface, which would not make proper contact with areas of rough skin. Using CNT as an array/forest on the surface of the electrode improved electrical contact by allowing penetration of the outer layers of the skin (stratum corneum). However, they are limited as they cannot form good contacts through skin pores and hairs as CNTs are uniformly grown on the substrate without any gaps [38–40].

We have developed a dry electrode using pvCNT that has lower contact impedance than conventional wet electrodes [41–43]. This electrode is suitable for physiological and neurological signal acquisition with reduced noise. However, in our previously reported development, we noticed that the CNT is weakly attached with mechanically unstable adherence to the stainless steel (SS) substrate of the electrode. Here, we propose a new method to resolve this issue of the pvCNT by applying a conductive polymer, polypyrrole (PPy), to improve mechanical adherence strength while maintaining conductivity. PPy polymer was used in this work for its easy preparation process, environmental safety, and high electrical conductivity.

In this paper, we report a novel dry electrode of Patterned Vertically-aligned Carbon NanoTubes (pvCNT) coated with a conductive polymer (Polypyrrole, PPy) that increases the adherence of CNT pillars to the stainless-steel substrate. The paper demonstrates the improved electrode performance, after coating, with regard to capturing ECG signals in contrast to non-coated and commercial electrodes. The paper also presents a characterization of the coated pvCNT electrode using evaluation metrics such as electrical contact-skin impedance, long-term impedance stability, and ECG signal capture. This paper extends our preliminary findings [43] with detailed characterization and elaboration.

2. pvCNT Electrode Fabrication and Coating

2.1. pvCNT Fabrication

We have shown in previous work that the prototyped electrodes are developed such that the CNTs are grown in an aligned vertical pattern resulting in a bristle-like structure [41,42]. The pillar heights (~1.5 mm) are sufficient to measure the signal through hairy and rough areas of the skin. For this pvCNT electrode, we have used MWCNTs due to their electrical conductivity and mechanical properties [31]. The pvCNT was fabricated by a commercial CNT fabrication facility (NanoLab, Boston, MA, USA) as follows: Catalytic Chemical Vapour Deposition (C-CVD) technique was used for aligned CNT growth by depositing 10 nm of Al_2O_3, followed by 1–2 nm of iron using a sputtering process through holes of a mask that was developed and imaged using photoresist to form the patterned array. After stripping the resist, the nanotubes were grown on the patterned substrate using the thermal growth process in several steps: heating, annealing, growth, and cooling down. The catalyst film breaks into islands during the heating and annealing steps, and the diameter and the density of the carbon nanotubes will be defined. The substrate was quickly annealed at 500 °C, cooled down to the growth temperature, and then the substrate was loaded for CNT growth. The average outer diameters of the MWCNT strands were 30 $\pm$ 15 nm. The array of pvCNT pillars were grown on a circular stainless-steel substrate with a diameter of 10 mm and thickness of 50 µm. Each pillar had a square base of 100 µm on each side.

The spacing between the pillars was 200 µm in all directions. Other spacings (50 and 100 µm) have been studied and tested in previous work but will not be investigated and tested here as they would expected to perform similarly. The schematic design, photograph and scanning electron microscopy (SEM) images of the pvCNTs, are depicted in Figure 1. Note that the top view of the pillars shows that the pillars slightly twist and bend over the height (~1 mm) which is expected for this extreme height of CNT fibers. Figure 1d shows the pillar top corner consisting of many CNT strands grouped tightly and vertically. SEM images of the pvCNT electrode were captured at the Integrated Microscopy Center (IMC), The University of Memphis (Memphis, TN, USA).

2.2. PPy Coating Procedure

Coating is the second step of sensor fabrication, as we proved before, and the strength of adhesiveness of the pvCNT pillars can be improved using a conductive polymer, polypyrrole (PPy). PPy can be changed from an electrical isolator to a good conductor using electrochemical procedures [19]. A liquid PPy from Sigma Aldrich (product number 482552) was used in this experiment. Many researchers have used PPy for coating biosensors [5]. We have used pvCNT electrodes with 200 µm spacing for this study. The pvCNT was prepared by applying 10 µL of 70% ethyl alcohol in order to decrease the surface tension of the CNT. Then, 10 µL of the PPy was added to the electrode and left until the entire substrate was covered. The prepared electrode was then dried using a preheated gun at 300 °C at distance of 10 cm for 30–60 s. Figure 2 shows the pvCNT electrode before (left) and after (right) the coating procedure. As evidenced in this figure, the size of the pvCNT pillars shrinks after the coating due to the high surface tension and viscosity of the PPy.

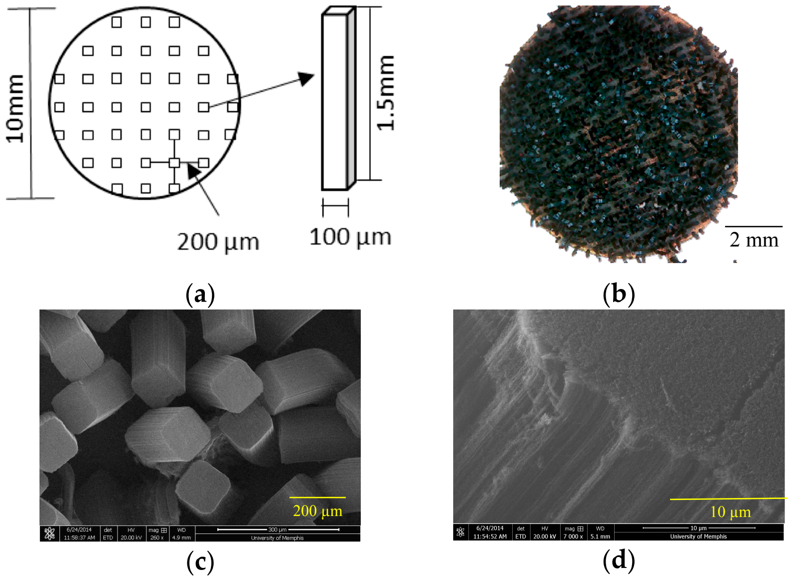

Figure 1. (**a**) Schematic design of the pillar and the pattern of patterned vertically-aligned Carbon NanoTubes (pvCNT) growth on stainless steel substrate. (**b**) Optical microscope image of a pvCNT electrode (200 µm spacing). (**c**) Scanning electron microscope (SEM) image (top view) of a pvCNT electrode (200 µm spacing) showing the pillars formed with vertically aligned CNT fibers. (**d**) SEM image of the top corner of a pillar.

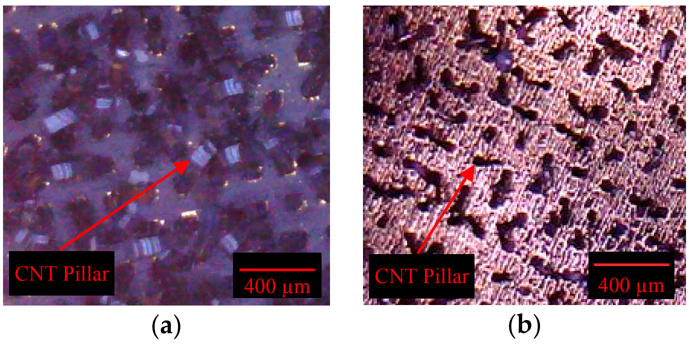

Figure 2. Images of pvCNT electrode without and with polypyrrole (PPy) coating. (**a**) Prior to PPy coating. (**b**) After PPy coating.

3. Experimental Method and Setup

3.1. PPy-coated pvCNT Electrode Conductivity Measurement

The conductivity of the electrode was analyzed by measuring its surface impedance. An Agilent 4294A Precision Impedance analyzer (Agilent Technologies Inc., Santa Clara, CA, USA) was used to analyze the impedance of coated and non-coated pvCNT electrodes using Dielectric Fixture 16451B at room temperature (~23 °C). The measurement data over time was automatically recorded using a Visual Basic script and analyzed using Microsoft Excel (Microsoft Corp, Redmond, WA, USA) and MATLAB (MathWorks, Natick, MA, USA). Measurement of the impedance of the pvCNT electrode was collected using Agilent Fixture 16451B ensuring the two plates were barely in contact with the substrate and the CNTs tips (stopping at a single click of the torque knob).

3.1.1. Impedance Measurement before and after Coating

Dielectric Fixture 16451B was attached to the Agilent Impedance Analyzer (IA) and used to measure the impedance of the coated and non-coated pvCNT electrodes. To ensure accurate measurements, the fixture was compensated and calibrated as per the manufacturer's instructions. All measurements were recorded at a frequency range of 40 Hz to 100 kHz.

3.1.2. Long-Term Impedance Measurement

In previous work, we showed that the impedance of pvCNT was stable over a long period of time. In this experiment, the coated and non-coated pvCNT impedances were monitored for 24 h. The data was automatically collected and transferred to the PC every hour. Figure 3a shows the impedance measurement equipment used.

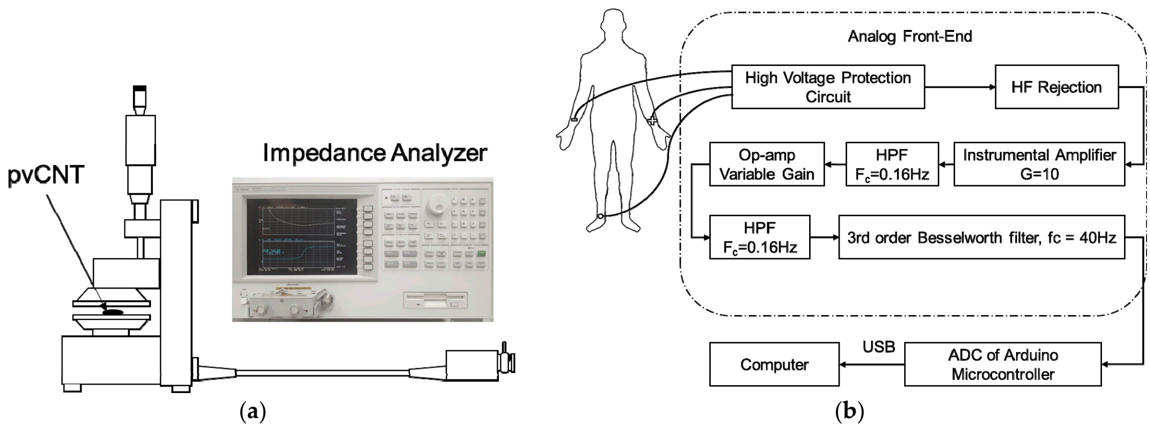

Figure 3. (**a**) Impedance measurement setup using Fixture 16451B attached to the Agilent 4294A Impedance Analyzer. (**b**) The block diagram of the AFE of the OLIMEX shield that are connected to the Arduino board and then to the computer through a USB cable.

3.2. *In Vitro Signal Capture*

Half-cell potential is one factor that affects the bio-signal quality as the half-cell potential appears at the interface of the electrode due to gel diffusion and shows up as a direct current (DC) offset. We have shown that the half-cell potential for the pvCNT electrode interfaced with Al foils is very small (~15 mV). Similar experiments were conducted to measure the half-cell potential of the coated pvCNT where a signal from a function generator was applied to the Al foil, captured using the coated pvCNT and then compared to the previous results for non-coated pvCNT and the commercial GS-26.

3.3. *Peel-Off Tests*

The peel test was conducted to measure the adhesion and tensile strength of the pvCNT pillar with the substrate. Drafting tape was attached to the top surface of the pvCNT and then peeled off slowly at a ~45° angle while the substrate was held and fixed with double-sided tape. A mini-digital microscope camera (Vividia 2.0MP Handheld USB Digital Microscope, Oasis Scientific Inc., Taylors, SC, USA) was used to inspect the samples before and after each test.

3.4. *In Vivo ECG Signal Capture*

The performance of the pvCNT electrode was investigated by recording ECG signals and comparing the quality of the signal measured to signals from traditional wet electrodes Ag/AgCl. An open source commercial hardware EKG/EMG shield (OLIMEX Ltd., Plovdiv, Bulgaria) was used to capture ECG signals. The shield EKG/EMG converts the analog differential signal attached to

CH1_IN+/CH1_IN− inputs into a single stream of data as output. The output signal is discretized via dedicated ADC embedded in the MCU onboard attached to the shield. The analog front end of the shield contains multiple stages as follows: a high voltage protection circuit, high frequency and noise rejection, an instrumental amplifier with a gain of 10, a high pass filter with a cutoff frequency of 0.16 Hz, an operational amplifier with variable gain (a gain of 80 was used), another high pass filter at same cutoff frequency, and a third order Besselworth filter with a cutoff frequency at 40 Hz and a gain of 3.56. The total applied gain was around 2848. Figure 3b shows the block diagram of the shield. The output signal was attached to the Arduino LEONARDO (Arduino LLC) board and digitized using 10-bit ADC with a sampling rate of 256 Hz then transferred to a computer using micro-USB for further digital processing. A Tektronix oscilloscope was used to monitor and visualize the ECG signal before recording.

The pvCNT electrode was attached to a flexible PCB (flex-PCB) on an exposed Cu pad with a diameter of 10 mm, to provide a low impedance, using double sided z-axis conductive tape (Electrically Conductive Adhesive Transfer Tape 9703, 3M Company, St. Paul, MN, USA). The flex-PCB was designed and prototyped at Cirexx Intl., Santa Clara, CA, USA. Three electrodes were placed on the human body at three positions: the left forearm, right forearm, and right leg. All of the measurements of the ECG signals were conducted at room temperature with no skin preparation. The ECG data was collected and recorded using the serial port and analyzed using MATLAB.

Figure 4a shows the setup of the pvCNT and the placement of the electrode on the left arm using a rubber band to ensure excellent skin-electrode contact during any body motions. Figure 4b shows the OLIMEX EKG/EMG shield attached to Arduino board. This study used the approved Institutional Review Board (IRB) protocol number 4212 (University of Memphis).

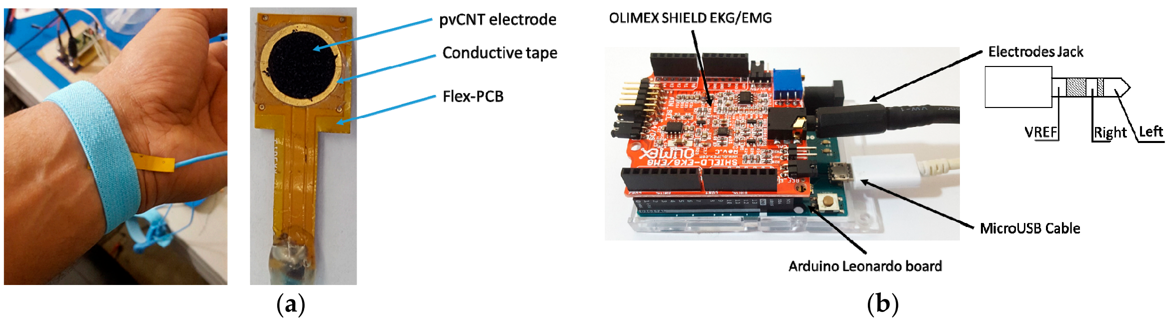

Figure 4. In vivo electrocardiogram (ECG) signal capture setup. (**a**) The pvCNT setup attached to the left arm. (**b**) The SHIELD_EKG_EMG attached with the Arduino Leonardo board.

4. Experimental Results

4.1. PPy-Coated pvCNT Electrode Conductivity Measurement Results

This section provides a summary of the data captured using the methods described above. All the impedance values in this paper are represented in terms of the amplitude and the phase angle.

4.1.1. Impedance Measurement Results Before and After Coating

Figure 5 shows the short-term impedance where the left shows the magnitude impedance (|Z|) for pvCNT with 200 μm spacing with and without PPy coating, and the right plot shows the phase angle of the impedance for the same electrodes. As expected, the impedance of the PPy-coated pvCNT increased by the impedance of the PPy film. For instance, the impedance of non-coated and PPy-coated pvCNT was 8.15 and 19.4 Ω, respectively, at 40 Hz. However, this higher impedance is well below gel electrode impedance and suitable for low noise impedimetric signal sensing. The phase shift of the coated pvCNT was also increased in the negative direction, possibly due to extra capacitance from to PPy coating.

The impedance of the coated and non-coated electrodes was observed at different frequencies. Particularly, the variation of the amplitude of the impedance for a non-coated electrode from 40 Hz to 100 kHz was 0.24 Ω, whereas for the coated electrode, the variation was around 0.1 Ω. While the variation of the phase for the non-coated and coated electrodes was less than 0.5°.

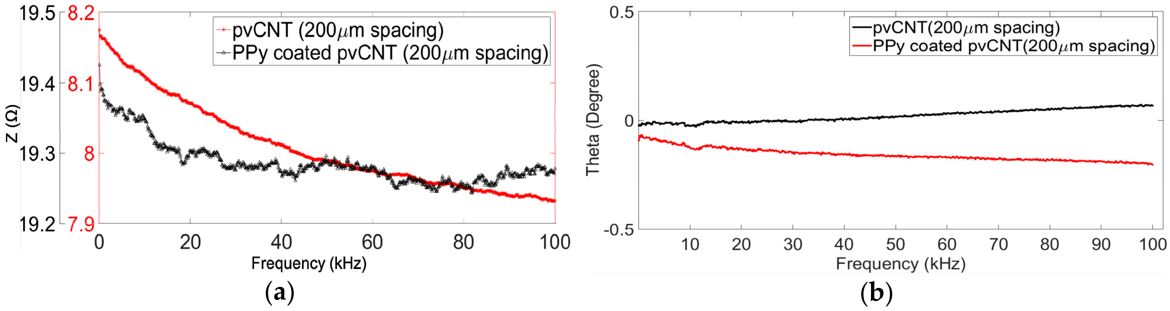

Figure 5. The amplitude (**a**) and phase (**b**) of the impedance for non-coated and PPy-coated pvCNT electrodes.

4.1.2. Long-Term Impedance Measurement Results

The impedance data was captured for frequencies from 40 Hz to 100 kHz. The measurements for the coated pvCNT at two different frequencies (40 Hz and 10 kHz) are shown in Figure 6. The results show that the amplitude and phase of the impedance of the coated electrode change very slightly within a range of 5 Ω and 1°, respectively, over 24 h. The amplitude impedance of the coated pvCNT was increased due to the PPy added to the electrode where the average impedance was around 20 Ω.

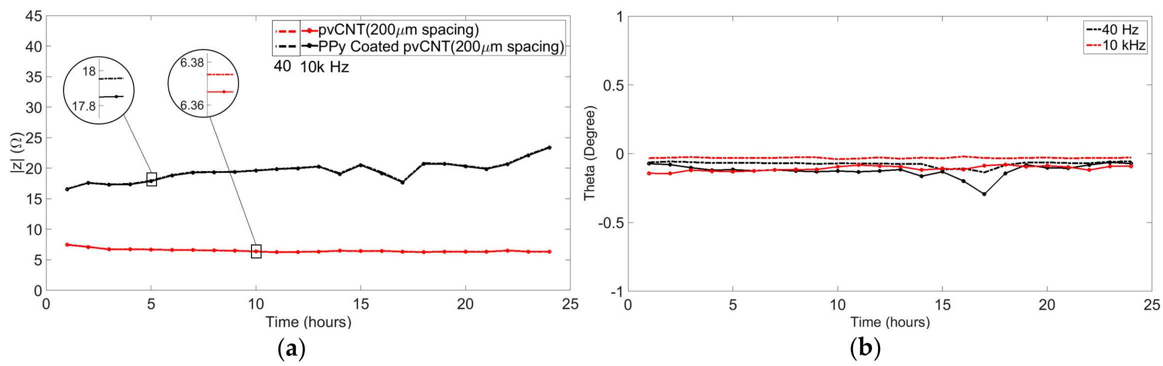

Figure 6. The amplitude (**a**) and phase (**b**) of the impedance of non-coated pvCNT electrode and PPy-coated pvCNT electrode for a long duration of 24 h.

It is noted that the impedance of PPy-coated pvCNT is higher than the non-coated version for all frequencies and might fluctuate over time. This is due to the extra impedance of the PPy (polymer) that is added to the impedance of the CNT pillars [17]. PPy impedance is also dependent on the environment (humidity, temperature, etc.). The coated electrode resistance is a combination of the resistance of the non-coated electrode and the resistance of PPy layer. Hence, depositing a thin film is important to reduce change of resistance. In our experiments, the typical change in resistance was only 5 Ω.

4.2. In Vitro Signal Capture Results

Experimental results show that the half-cell potential of the coated pvCNT interfacing with Al foil is 1.3 mV. On the other hand, the potential drops of the pvCNT non-coated and GS-26 electrodes, shown in our previous work [29], were 15 mV and 809.4 mV, respectively.

Due to gel diffusion, the potential offset drops on Ag/AgCl were high compared to other electrodes. The applied signal was sinusoidal with a frequency of 100 Hz. Figure 7a shows a snapshot of the captured signal and Figure 7b shows the different potential drops of each electrode. Due to the polarization that occurred at the interface, a small electric field would rise, shown as a potential offset. Furthermore, the equivalent circuit of the electrode is an RC in parallel, hence, the captured signal will have some phase shift due to the capacitance component.

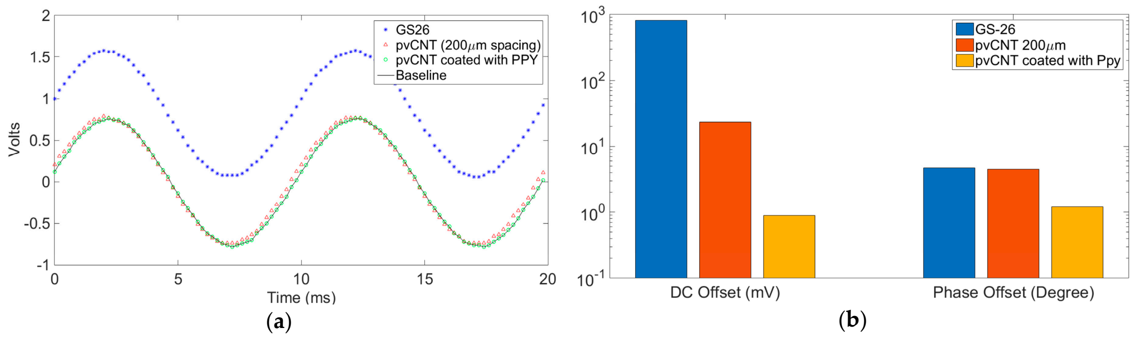

Figure 7. In vitro test results of the electrodes. (**a**) Signal capture by coated and non-coated pvCNT dry electrodes compared to the commercial gel GS-26 electrodes interfaced with Al foil. (**b**) Plots comparing DC offset voltages and phase offsets of these electrodes.

4.3. Peel-Off Test Results

Mechanical peel-off tests were performed to check how strongly the CNT pillars were attached to the SS substrate. Figure 8 shows the microscopy images of the non-coated and coated pvCNT electrodes prior to and after the peel-off test experiments. As shown in Figure 8b, the amount of CNT pillars stuck to the drafting tape was significantly fewer for coated electrodes than for the non-coated electrodes shown in Figure 8a. These results show that the CNT pillars of the PPy-coated pvCNT electrodes are attached more strongly than the non-coated electrodes. Drying the PPy after spreading it uniformly through the CNT pillars makes an adhesion layer between the bases of the pillars and the substrate.

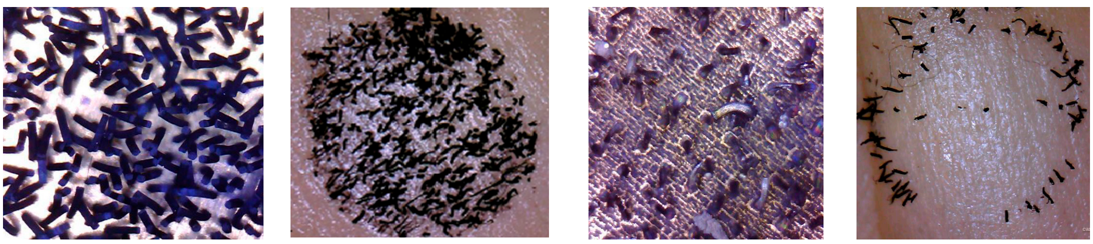

(**a**) Non coated pvCNT (**b**) Coated pvCNT

Figure 8. Microscopy images of pvCNT prior to and after the peel-off experiments. (**a**) A non-coated pvCNT electrode prior to the test and the residue left on the tape after the test. (**b**) PPy-coated pvCNT electrode prior to the test and the residue left on the tape after the test.

4.4. In Vivo ECG Signal Capture Results

Figure 9 shows the ECG signal acquired using the traditional wet electrodes Ag/AgCl (top) and the pvCNT PPy-coated electrode (bottom) described in this work. The pvCNT measurements are very similar to traditional wet electrode measurements. The typical ECG characteristics (QRS-complex, P-wave, and T-wave) were clearly visible as shown in Figure 9. The P-wave comes before the QRS-complex which is then followed by the T-wave [1]. The heart rate, in this case, was around 78 beats per minute. Optical images were taken after the experiments to show how many carbon nanotubes had detached and stuck to the skin. Figure 10 shows that the PPy-coated pillars are stable and strongly adhered to the stainless-steel substrate.

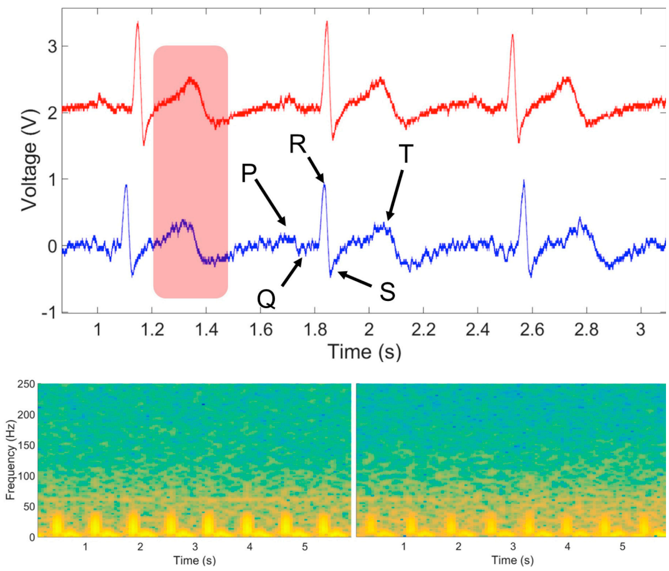

Figure 9. The ECG signal collected by two electrodes for comparison (Red) Commercial gel electrode, GS-26, and (Blue) PPy coated pvCNT. (Bottom) Time-frequency analysis (Left: GS-26, Right: PPy coated pvCNT) show similar performance and noise characteristics.

Figure 10. Photographs showing the PPy-coated pvCNT after the ECG signal capture experiments.

5. Conclusions

In previous work, we have shown the feasibility of using a novel dry electrode (pvCNT) for physiological and neurological bioelectric or impedimetric signal capturing. The results showed stable and low impedance for short and long periods compared to conventional electrodes. The CNT-based electrodes were fabricated using MWCNT grown in a pillar pattern and vertically aligned on a stainless-steel circular substrate with a diameter of 10 mm. These pillars were weakly attached to the substrate. An electrically conductive polymer polypyrrole (PPy) was used in this study to improve the mechanical stability of the CNT pillars in the pvCNT electrodes. The PPy-coated pvCNTs showed that the impedance of the electrode has increased but the electrodes had a more stable and stronger mechanical adhesion to the SS substrate. In addition, this polymer decreases the toxicity of the CNT making it safer for use on skin. The capability of using the improved pvCNT for monitoring and recording the ECG signals was investigated and the results were compared with commercial gel ECG electrodes (Ag/AgCl). Although the collected ECG signals using pvCNT had more noise (typical for dry ECG electrodes), the typical ECG signal characteristics components, including the P-wave, T-wave, and QRS complex were clearly identifiable and observed.

Author Contributions: Conceptualization, B.I.M.; Methodology, M.A. and B.I.M.; Software, M.A.; Validation, M.A.; Investigation, M.A.; Resources, M.A. and B.I.M.; Data Curation, M.A.; Writing-Original Draft Preparation, M.A.; Writing-Review & Editing, M.A. and B.I.M.; Visualization, M.A.; Supervision, B.I.M.; Project Administration, B.I.M.

Funding: This research received no external funding.

Conflicts of Interest: The authors declare no conflict of interest.

References

1. Yazicioglu, R.F.; VanHoof, C.; Puers, R. *Bio-Potential Readout Circuits for Portable Acquisition Systems*; Springer: Berlin, Germany, 2008.
2. Thakor, N.V. Biopotentials and Electrophysiology Measurement. In *The Measurement, Instrumentation and Sensors Handbook*; CRC Press: Boca Raton, FL, USA, 1999.
3. Martinsen, O.G.; Grimnes, S. *Bioimpedance & Bioelectricity Basics*; Academic Press: Bodmin, UK, 2000.
4. Plonsey, R.; Barr, R.C. *Bioelectricity: A Quantitative Approach*, 3rd ed.; Springer: New York, NY, USA, 2007.
5. Patel, S.; Park, H.; Bonato, P.; Chan, L.; Rodgers, M. A review of wearable sensors and systems with application in rehabitation. *J. Neuroeng. Rehabil.* **2012**, *9*, 17. [CrossRef] [PubMed]
6. Lin, C.T.; Liao, L.D.; Liu, Y.H.; Wang, I.J.; Lin, B.S.; Chang, J.Y. Novel dry polymer foam electrodes for long-term EEG measurement. *IEEE Trans. Biomed. Eng.* **2011**, *58*, 1200–1207. [PubMed]
7. Searle, A.; Kirkup, L. A direct comparison of wet, dry and insulating bioelectric recording electrodes. *Physiol. Meas.* **2000**, *21*, 271–283. [CrossRef] [PubMed]
8. Chi, Y.M.; Jung, T.G.; Cauwenberghs, G. Dry-contact and noncontact biopotential electrodes: Methodological review. *IEEE Rev. Biomed. Eng.* **2010**, *3*, 106–119. [CrossRef] [PubMed]
9. Gurger, C.; Krausz, G.; Allison, B.Z.; Edlinger, G. Comparison of dry and gel based electrodes for P300 brain-computer interfaces. *Front. Neurosci.* **2012**, *6*, 1–7.
10. Huigen, E.; Peper, A.; Grimbergen, C.A. Investigation into the origin of the noise of surface electrodes. *Med. Biol. Eng. Comput.* **2002**, *40*, 332–338. [CrossRef] [PubMed]
11. Webster, J. *Medical Instrumentation: Application and Design*; John Wiley & Sons: Hoboken, NJ, USA, 1998.
12. Ruffini, G.; Dunne, S.; Farres, E.; Marco-Pallares, J.; Ray, C.; Mendoza, E.; Silva, R.; Grau, C. A dry electrophysiology electrode using CNT arrays. *Sens. Actuators A Phys.* **2006**, *132*, 34–41. [CrossRef]
13. Alemdar, H.; Ersoy, C. Wireless sensor networks for healthcare: A survey. *Comput. Netw.* **2010**, *54*, 2688–2710. [CrossRef]
14. He, B.; Coleman, T.; Genin, G.M.; Hu, X.; Johnson, N.; Liu, T.; Makeig, S.; Sajda, P.; Ye, K. Grand challenges in mapping the human brain: NSF workshop report. *IEEE Trans. Biomed. Eng.* **2013**, *60*, 2983–2992. [PubMed]
15. Baek, J.; An, J.; Choi, J.; Park, K.; Lee, S. Flexible polymeric dry electrode for long-term monitoring of ECG. *Sens. Actuators A. Phys.* **2008**, *143*, 423–429. [CrossRef]
16. Wang, L.; Liu, J.; Yang, B.; Yang, C. PDMS based low cost flexible dry electrode for long-term EEG measurement. *IEEE Sens. J.* **2012**, *12*, 2898–2904. [CrossRef]
17. Jamadade, S.; Jadhav, S.; Puri, V. Electromagnetic properties of polypyrrole thin film on copper substrate. *Phys. Res.* **2010**, *1*, 205–210.
18. Chiou, J.C.; Ko, L.W.; Lin, C.T.; Hong, C.T.; Jung, T.P.; Liang, S.F.; Jeng, J.L. Using novel MEMS EEG sensors in detecting drowsiness application. In Proceedings of the Biomedical Circuits and Systems Conference, London, UK, 29 November–1 December 2006; pp. 33–36.
19. Matthews, R.; Turner, P.J.; McDonald, N.J.; Ermolaev, K.; Mc Manus, T.; Shelby, R.A.; Steindorf, M. Real time workload classification from an ambulatory wireless EEG system using hybrid EEG electrodes. In Proceedings of the 2008 30th Annual International Conference of the IEEE Engineering in Medicine and Biology Society, Vancouver, BC, Canada, 20–25 August 2008; pp. 5871–5875.

20. Grozea, C.; Voinescu, C.D.; Fazli, S. Bristle-sensors—Low-cost flexible passive dry EEG electrodes for neurofeedback and BCI applications. *J. Neural Eng.* **2011**, *8*, 025008. [CrossRef] [PubMed]
21. Gruetzmann, A.; Hansen, S.; Muller, J. Novel dry electrodes for ECG monitoring. *Physiol. Meas.* **2007**, *28*, 1375–1390. [CrossRef] [PubMed]
22. Gondran, C.; Siebert, E.; Fabry, P.; Novakov, E.; Gumery, P.Y. Non-polarisable dry electrode based on NASICON ceramic. *Med. Biol. Eng. Comput.* **1995**, *33*, 452–457. [CrossRef] [PubMed]
23. Xie, L.; Geng, Y.; Mäntysalo, M.; Xu, L.L.; Jonsson, F.; Zheng, L.R. Heterogeneous Integration of Bio-Sensing System-on-Chip and Printed electronics. *IEEE J. Emerg. Sel. Top. Syst.* **2012**, *2*, 672–682. [CrossRef]
24. Kumar, P.S.; Rai, P.; Oh, S.; Kwon, H.; Varadan, V.K. Flexible capacitive electrodes using carbon nanotube and acrylic polymer nanocomposites for healthcare textiles. *Smart Nanosyst. Eng. Med.* **2012**, *2*, 18–24.
25. Lee, J.M.; Pearce, F.; Hibbs, A.D.; Matthews, R.; Morrissette, C. Evaluation of a capacitively-coupled, non-contact (through clothing) electrode or ECG monitoring and life signs detection for the objective force warfighter. In Proceedings of the Combat Casualty Care in Ground Based Tactical Situations: Trauma Technology and Emergency Medical Procedures, DTIC Document, St. Pete Beach, FL, USA, 16–18 August 2004.
26. Zhou, Y.; Ding, X.; Zhang, J.; Duan, Y.; Hu, J.; Yang, X. Fabrication of conductive fabric as textile electrode for ECG monitoring. *Fibers Polym.* **2014**, *15*, 2260–2264. [CrossRef]
27. Yapici, M.K.; Alkhidir, T.; Samad, Y.A.; Liao, K. Graphene-clad textile electrodes for electrocardiogram monitoring. *Sens. Actuators B Chem.* **2015**, *221*, 1469–1474. [CrossRef]
28. Sullivan, T.J.; Deiss, S.R.; Cauwenberghs, G.; Jung, T. A low-noise, low-power EEG acquisition node for scalable brain-machine interfaces. *SPIE Bioeng. Bioinspir. Syst. III* **2007**, *6592*, 659203.
29. Ha, S.; Kim, C.; Chi, Y.M.; Akinin, A.; Maier, C.; Ueno, A.; Cauwenberghs, G. Integrated circuits and electrode interfaces for noninvasive physiological monitoring. *IEEE Trans. Biomed. Eng.* **2014**, *61*, 1522–1537. [PubMed]
30. Zhang, Y.; Bai, Y.; Yan, B. Functionalized carbon nanotubes for potential medicinal applications. *Drug Discov. Today* **2010**, *15*, 428–435. [CrossRef] [PubMed]
31. White, C.T.; Todorov, T.N. Carbon nanotubes as long ballistic conductors. *Nature* **1998**, *393*, 240–243. [CrossRef]
32. Tran, T.Q.; Headrick, R.J.; Bengio, E.A.; Myo Myint, S.; Khoshnevis, H.; Jamil, V.; Duong, H.M.; Pasquali, M. Purification and Dissolution of Carbon Nanotube Fibers Spun from the Floating Catalyst Method. *ACS Appl. Mater. Interfaces* **2017**, *9*, 37112–37119. [CrossRef] [PubMed]
33. Bareket-Keren, L.; Hanein, Y. Carbon nanotube-based multi electrode arrays for neuronal interfacing: Progress and prospects. *Front. Neural Circuits* **2013**, *6*, 1–60. [CrossRef] [PubMed]
34. Smart, S.K.; Cassady, A.I.; Lu, G.Q.; Martin, D.J. The biocompatibility of carbon nanotubes. *Carbon* **2006**, *44*, 1034–1047. [CrossRef]
35. Chlopek, J.; Czajkowska, B.; Szaraniec, B.; Frackowiak, E.; Szostak, K.; Beduin, F. In vitro studies of carbon nanotubes biocompatibility. *Carbon* **2006**, *44*, 1106–1111. [CrossRef]
36. Ruffini, G.; Dunne, S.; Farres, E.; Watts, P.C.P.; Mendoza, E.; Silva, S.R.P.; Grau, C.; Marcho-Pallares, J.; Fuentemilla, L.; Vandecasteele, B. ENOBIO—First tests of a dry electrophysiology electrode using carbon nanotubes. In Proceedings of the 2006 International Conference of the IEEE Engineering in Medicine and Biology Society, New York, NY, USA, 30 August–3 September 2006; pp. 1826–1829.
37. Ruffini, G.; Dunne, S.; Fuentemilla, L.; Grau, C.; Farres, E.; Marco-Pallares, J.; Watts, P.C.P.; Silva, S.R.P. First human trials of a dry electrophysiology sensor using a carbon nanotube array interface. *Sens. Actuators A Phys.* **2008**, *144*, 275–279. [CrossRef]
38. Radhakrishana, J.K.; Bhusan, H.; Pandian, P.S.; Rao, K.U.B.; Padaki, V.C.; Aatre, K.; Xie, J.; Abraham, J.K.; Varadan, V.K. Growth of CNT array, for physiological monitoring applications. *Proc. SPIE* **2008**, *6931*, 69310.
39. Baskey, H.B. Development of carbon nanotube based sensor for wireless monitoring of electroencephalogram. *DRDO Sci. Spectr.* **2009**, *59*, 161–163.
40. Jung, H.; Moon, J.; Baek, D.; Lee, J.; Choi, Y.; Hong, J.; Lee, S. CNT/PDMS composite flexible dry electrodes for long-term ECG monitoring. *IEEE Trans. Biomed. Eng.* **2012**, *59*, 1472–1479. [CrossRef] [PubMed]
41. Abu-Saude, M.; Consul-Pacareu, S.; Morshed, B.I. Feasibility of Patterned Vertical CNT for Dry Electrode Sensing of Physiological Parameters. In Proceedings of the 2015 IEEE Topical Conference on Biomedical Wireless Technologies, Networks, and Sensing Systems (BioWireleSS), San Diego, CA, USA, 25–28 January 2015; pp. 1–4.

42. Abu-Saude, M.; Morshed, B.I. Patterned Vertical Carbon Nanotube (pvCNT) Dry Electrodes for Impedimetric Sensing and Stimulation. *IEEE Sens. J.* **2015**, *15*, 5851–5858. [CrossRef]
43. Abu-Saude, M.; Morshed, B.I. Polypyrrole (PPy) Conductive Polymer Coating of Dry Patterned Vertical CNT (pvCNT) Electrode to Improve Mechanical Stability. In Proceedings of the IEEE Topical Conf. Biomedical Wireless Technologies, Networks, and Sensing Systems (BioWireleSS), Austin, TX, USA, 24–27 January 2016; pp. 84–87.